Automatic control of convertible fixed-wing drones with vectorized thrust

André Anglade, Jean-Marie Kai, Tarek Hamel, Claude Samson

Automatic control of convertible fixed-wing drones with vectorized thrust

André Anglade, Jean-Marie Kai, Tarek Hamel and Claude Samson

***Abstract*— This paper proposes a control design strategy, encompassing trajectory tracking and path following, for a category of convertible aircraft with fixed wings and vectorized thrust, as exemplified by the *Harrier* jet aircraft and the *V-22 Osprey*. The approach relies on, and extends, previous works on the control of hovering vehicles (helicopters, quadrotors,...), axisymmetric devices (rockets, missiles,...), and fixed-wing aircraft (airplanes). In particular it exploits a common nonlinear model of aerodynamic forces exerted on the vehicle, both simple and representative of the underlying physics. Besides the unifying property of this approach, the proposed solution addresses the delicate transition problem between hovering and cruising flight, and thus the concomitant thrust tilting issue, in a novel manner with the possibility of continuously minimizing the thrust intensity, and thus energy expenditure.**

I. Introduction

Convertible aircraft endowed with wings are vehicles that can hover, like helicopters, and also take advantage of airspeed-induced lift forces to cruise at high speeds with reduced energy expenditure, and thus good flight autonomy. They can be classified into three main categories: tail-sitters with fixed wings and fixed thrust direction (of which the Convair XFY-1 and Snecma Coléoptère are historical prototypes), tilt rotor-and-wing aircraft with thrust direction and wings pivoting jointly (Hiller X-18, LTV XC-142, Canadair CL-84), and fixed-wing aircraft with vectorized thrust (Bell-Boeing V-22 Osprey, Bell XV-15 and V-280 Valor). Nowadays, all three categories are well represented in the rapidly expanding market of small drones. While encompassing the cases of classical fixed-wing aircraft and multirotor VTOLs, the present paper addresses more specifically the control of convertible aircraft belonging to the third category.

Large convertible aircraft have been built and flown for decades, even though only a few of them passed the prototyping stage. Control design studies for Tilt-Rotor Unmanned Aerial Vehicles (TRUAVs), belonging to the aforementioned second and third categories, are more recent and constitute to this day a small portion of the specialized literature devoted to the control of UAVs (see [1], [2] for a review of these techniques up to the year 2015).

The flight of aircraft with vectorized thrust is commonly decomposed into three distinct modes, namely i) hovering (helicopter), ii) transitioning, and iii) cruising (airplane). In the first mode the rotor axes are oriented perpendicularly to the aircraft body, whereas in the third mode they are aligned with the aircraft body. Most of the control literature about aerial vehicles is devoted to these two classical modes [2]. The transition between them, involving thrust direction modification, has been little studied on a theoretical ground [3]. This transition is typically performed by implementing an *ad hoc* scheduling policy, when the aircraft moves horizontally and reaches a certain airspeed, either during an acceleration phase (hovering to cruising) or during a deceleration (cruising to hovering). A common practice is to modify the thrust tilt angle in relation to the airspeed [1], [4]–[6]. Taking advantage of the thrust tilting degree of freedom to minimize the thrust intensity is evoked in [7] as a perspective worth to be investigated. This possibility, and a generalized scheduling policy, are addressed in the present paper within a unified control approach that encompasses our previous work on *trajectory tracking* [8] and *path following* [9], [10] for conventional fixed-wing aircraft. The proposed control design exploits a generic nonlinear model of aerodynamical forces applied to the aircraft whose main asset is to be representative of the physics underlying the creation of the environmental forces, and enough simple to allow for a nonlinear control design lending itself to convergence and stability analyses.

The paper is organized as follows. Section II recalls the equations of motion of an aircraft, and presents the model of applied aerodynamic forces subsequently used for control design. Section III describes the three stages of the proposed control design, with its adaptation to either trajectory tracking or path following objectives. For the sake of genericity, and in order to be as much independent as possible of specific means of actuation, the thrust's intensity and tilting angle, and the aircraft angular velocity are used as intermediary control inputs. Lyapunov convergence and stability of the proposed feedback control laws can be proved by adapting the analyses reported in [8] and [10]. This analysis is not reported here due to space limitations. Application to a particular class of convertible aircraft is worked out in Section IV by considering the case of a quad tilt-rotor fixed-wing aircraft and by specifying the control allocation for the production of the required thrust and torques. Hardware-in-the-loop simulation results are reported in Section V, and concluding remarks are given in the last Section VI.

II. Control model

A. Notation

- $\boldsymbol{E}^3$ denotes the $3D$ Euclidean vector space associated with the inertial frame $\mathcal{I} = \{O; \boldsymbol{i}_0, \boldsymbol{j}_0, \boldsymbol{k}_0\}$, with $\boldsymbol{k}_0$ pointing vertically and downward.

A. Anglade and J.M. Kai are with I3S, Université Côte d'Azur, CNRS, Sophia Antipolis, France, $aanglade(kai)@i3s.unice.fr$.

T. Hamel is with I3S and Institut Universitaire de France, Université Côte d'Azur, CNRS, Sophia Antipolis, France, $thamel@i3s.unice.fr$.

C. Samson (corresponding author) is with INRIA and I3S, Université Côte d'Azur, CNRS, Sophia Antipolis, France, $claude.samson@inria.fr$, $csamson@i3s.unice.fr$.

- Vectors in $\boldsymbol{E}^3$ are written with bold letters. Inner and cross products in $\boldsymbol{E}^3$ are denoted by the symbols $\cdot$ and $\times$ respectively. Ordinary letters are used for real vectors of coordinates, and the $ith.$ component of a real vector x is denoted as x_i.
- When $x \in \mathbb{R}^n$ (resp. $\boldsymbol{x} \in \boldsymbol{E}^3$), $|x|$ (resp. $|\boldsymbol{x}|$) denotes the Euclidean norm of x (resp. $\boldsymbol{x}$). Of course, $|x| = |\boldsymbol{x}|$.
- $\Pi_{\boldsymbol{u}}$ denotes the operator of projection on the plane orthogonal to $\boldsymbol{u}$.
- G denotes the aircraft center of mass (CoM).
- $\mathcal{B} = \{G; \boldsymbol{\imath}, \boldsymbol{\jmath}, \boldsymbol{k}\}$ is the chosen aircraft-fixed frame, with $\boldsymbol{\imath}$ and $\boldsymbol{\jmath}$ parallel to the so-called zero-lift plane of the aircraft. We assume that this latter plane is not affected by thrust direction changes. This implies in particular that the aircraft is designed so as to minimize aerodynamic interference between the propulsion system and the main wing. The vector $\boldsymbol{\imath}$ (resp. $\boldsymbol{\jmath}$) is along the longitudinal (resp. lateral) axis of the aircraft (see Fig. 1).
- $\boldsymbol{l} = \sin(\theta)\boldsymbol{\imath} - \cos(\theta)\boldsymbol{k}$ is the unitary vector characterizing the thrust direction, with θ the tilting thrust angle.
- $\boldsymbol{\omega}$ is the angular velocity of $\mathcal{B}$ w.r.t. $\mathcal{I}$, i.e.

$$\frac{d}{dt}(\boldsymbol{\imath}, \boldsymbol{\jmath}, \boldsymbol{k}) = \boldsymbol{\omega} \times (\boldsymbol{\imath}, \boldsymbol{\jmath}, \boldsymbol{k}) \tag{1}$$

  The vector of coordinates of $\boldsymbol{\omega}$ in the body-fixed frame $\mathcal{B}$ is denoted as ω.
- m is the body mass.
- $\boldsymbol{p}$ is the CoM position w.r.t. the inertial frame.
- $\boldsymbol{v}$ is the CoM velocity w.r.t. the inertial frame, i.e.

$$\dot{\boldsymbol{p}} = \boldsymbol{v} \tag{2}$$

  The vector of coordinates of $\boldsymbol{v}$ in the body-fixed frame $\mathcal{B}$ is denoted as v.
- $\dot{\boldsymbol{v}}$ is the CoM acceleration w.r.t. the inertial frame;
- $\boldsymbol{g} = g_0\,\boldsymbol{k}_0$ is the gravitational acceleration;
- $\boldsymbol{v}_w$ is the ambient wind velocity w.r.t. $\mathcal{I}$, which we assume bounded with first and second time-derivatives also bounded;
- $\boldsymbol{v}_a = \boldsymbol{v} - \boldsymbol{v}_w$ is the aircraft air-velocity. The vector of coordinates of $\boldsymbol{v}_a$ in the body fixed-frame $\mathcal{B}$ is denoted as v_a.
- The direction of $\boldsymbol{v}_a$ in the aircraft-fixed frame is characterized by two angles α and β such that

$$\boldsymbol{v}_a = |v_a|(\cos\alpha(\cos\beta\,\boldsymbol{\imath} + \sin\beta\,\boldsymbol{\jmath}) + \sin\alpha\,\boldsymbol{k}) \tag{3}$$

  $\alpha = \arcsin(v_{a,3}/|v_a|)$ and $\beta = \arctan(v_{a,2}/v_{a,1})$ denote the angle of attack and the sideslip angle respectively.

B. Control inputs and model equations

We assume that the control inputs consist of a thrust force $\boldsymbol{T} = T\boldsymbol{l}$, typically produced by propellers or jet turbines, and a torque vector $\boldsymbol{\Gamma}$. This torque is used to modify the vehicle's orientation at will. It can be produced in various ways by using tilting control surfaces (standard airplanes), differential multi-rotors speeds (classical multirotor drones), cyclic blade control (helicopters), a combination of tilting control surfaces with cyclic blade control (V-22 Osprey, Bell V-280 Valor), or a combination of tilting control surfaces with differential multi-rotors speeds (the quad tilt rotor aircraft represented in Fig. 1), etc. Due to the large number of possible configurations, and for the sake of genericity, the actuation system producing this torque is not specified in the first control design stages. More specifically, we assume the pre-existence of low level feedback loops that control the production of a torque vector ensuring the asymptotic stabilization of any desired angular velocity for the vehicle's body. This is a standard backstepping assumption. Under this assumption the body angular velocity $\boldsymbol{\omega}$ becomes an intermediate control variable. For the same reason, the controlled actuation in charge of stabilizing the thrust tilt angle at a desired value is not specified either. Under these assumptions and approximations, the control inputs here considered are the thrust intensity T, the thrust tilt angle θ, and the body angular velocity $\boldsymbol{\omega}$. The corresponding aircraft model equations are then reduced to the kinematic equations (1) and (2) complemented with Newton's equation

$$m\dot{\boldsymbol{v}} = m\boldsymbol{g} + \boldsymbol{F}_a + T(\sin(\theta)\boldsymbol{\imath} - \cos(\theta)\boldsymbol{k}) \tag{4}$$

with $\boldsymbol{F}_a$ denoting the resultant of the aerodynamic forces exerted on the vehicle. Prior to exploiting this latter equation for control design, a model of $\boldsymbol{F}_a$ is needed.

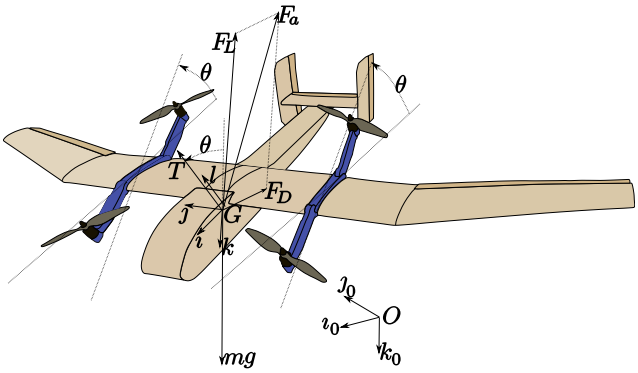

Fig. 1. Frames and forces

C. Aerodynamic forces

The resultant aerodynamic force $\boldsymbol{F}_a$ applied to a rigid body moving with air-velocity $\boldsymbol{v}_a$ is traditionally decomposed into the sum of a *drag* force $\boldsymbol{F}_D$ along the direction of $\boldsymbol{v}_a$ and a *lift* force $\boldsymbol{F}_L$ perpendicular to this direction, i.e.

$$\boldsymbol{F}_a = \boldsymbol{F}_D + \boldsymbol{F}_L \tag{5}$$

The intensities of drag and lift forces are essentially proportional to $|v_a|^2$ modulo variations characterized by two dimensionless functions C_D and C_L, which depend in the first place on the orientation of $\boldsymbol{v}_a$ w.r.t. the body, but also on the Reynolds number R_e and Mach number M. These dimensionless functions are called the *aerodynamic characteristics* of the body, or *drag coefficient* and *lift coefficient*

respectively. More precisely

$$\boldsymbol{F}_D = -\eta_a |v_a| C_D \, \boldsymbol{v}_a \ , \quad \boldsymbol{F}_L = \eta_a |v_a| C_L \, \boldsymbol{v}_a^\perp \tag{6}$$

with

- $\boldsymbol{v}_a^\perp$ some vector perpendicular to $\boldsymbol{v}_a$ and such that $|\boldsymbol{v}_a^\perp| = |v_a|$,
- $\eta_a := \frac{\rho \Sigma}{2}$ with ρ the *free stream* air density, and Σ an area germane to the body shape.

We neglect here the dependence of the aerodynamic characteristics on the Reynolds and Mach numbers. This is all the more justified for scale-model aircraft evolving at nearly constant altitudes and at speeds much lower than the speed of sound. The more specific model that we propose to use is:

$$\boldsymbol{F}_a = -\big(c_0 (\boldsymbol{v}_a \cdot \boldsymbol{\imath}) \boldsymbol{\imath} + \bar{c}_0 (\boldsymbol{v}_a \cdot \boldsymbol{k}) \boldsymbol{k}\big) |v_a| + (\boldsymbol{v}_a \cdot \boldsymbol{\jmath}) \boldsymbol{O}(\boldsymbol{v}_a) \tag{7}$$

with c_0 and c_1 denoting positive numbers, $\bar{c}_0 = c_0 + 2c_1$, and $\boldsymbol{O}(\boldsymbol{v}_a)$ any Euclidean vector-valued function such that the ratio $\frac{|\boldsymbol{O}(\boldsymbol{v}_a)|}{|v_a|}$ is bounded. This model was previously used in [8] and [9] for the design of control solutions in the case of classical fixed-wing aircraft. Note that i) this model encompasses the zero force assumption commonly made in the case of VTOL vehicles moving slowly ($c_0 = \bar{c}_0 = 0$, $\boldsymbol{O}(\boldsymbol{v}_a) = \boldsymbol{0}$), and ii) the non-dependence of this model upon the tilt angle θ is equivalent to assuming that modifications of the thrust direction do not (little, in practice) affect the aircraft aerodynamics. One easily verifies that this model is also compatible with the general relations (5) and (6), in particular when the lateral airspeed vanishes. In this latter case (7) yields $\boldsymbol{v}_a^\perp = -\frac{|v_a|}{\cos\alpha} \boldsymbol{k} - \tan\alpha \boldsymbol{v}_a$, $C_D(\alpha) = (c_0 + 2c_1 \sin^2\alpha)/\eta_a$, and $C_L(\alpha) = c_1 \sin 2\alpha / \eta_a$. For small angles of attack $|\alpha|$ the drag coefficient C_D is thus approximately equal to $\frac{c_0}{\eta_a}$ and the lift coefficient C_L is approximately proportional to the angle of attack with the coefficient of proportionality given by $\frac{2c_1}{\eta_a}$. This is coherent with experimental data performed on a variety of wing profiles and axisymmetric bodies [11]. Note also that, by contrast with other models, which are valid only locally for small angles of attack, the proposed model respects the physical property of no lift when the air-velocity is perpendicular to the aircraft zero-lift plane, i.e. when $\alpha = \pi/2$. This property is of particular interest for scale-model aircraft that are very sensitive to aerology conditions, and for convertible aerial vehicles whose angle of attack may vary in large proportions between hovering and cruising flight phases. Nevertheless, this model fails to account for the abrupt and complex stall phenomena occurring beyond some angle of attack (typically around $\alpha = \pi/10$). A way to tentatively overcome this shortcoming consists in modifying the coefficients c_0 and c_1 beyond the stall angle [11].

III. Control

For the sake of simplification, we here assume that the aircraft position, attitude, inertial velocity, and air velocity are either precisely measured or well estimated.

A. Design methodology

The proposed control design methodology involves three steps.

1) First step: This step consists in determining the expression of a feedback control function $\boldsymbol{\xi}$ that would achieve the desired objective(s) if the system dynamic equation was simply

$$\dot{\boldsymbol{v}} = \boldsymbol{\xi} \tag{8}$$

modulo slowly varying additive perturbations (conceptually representing modeling errors). For instance, consider the objective of having $\boldsymbol{v}$ converge robustly to a desired velocity $\boldsymbol{v}_r(t)$. Let $\boldsymbol{I}$ denote an adequate bounded integral of the velocity error $\tilde{\boldsymbol{v}} \equiv (\boldsymbol{v} - \boldsymbol{v}_r(t))$. Then a possible Proportional/Integral (PI) function $\boldsymbol{\xi}$ yielding the exponential stabilization at zero (in the sense of Lyapunov) of the extended state error $(\tilde{\boldsymbol{v}}, \boldsymbol{I})$ is

$$\boldsymbol{\xi}(\boldsymbol{v}, \boldsymbol{I}, t) = \dot{\boldsymbol{v}}_r(t) - k_v (\boldsymbol{v} - \boldsymbol{v}_r(t)) - k_I \boldsymbol{I},$$

with k_v and k_I denoting positive gains.

In the case of the *trajectory tracking* problem, the objective is to have the position $\boldsymbol{p}$ converge robustly to a desired position $\boldsymbol{p}_r(t)$. Let $\boldsymbol{I}$ denote an adequate bounded integral of the position error $\tilde{\boldsymbol{p}} \equiv \boldsymbol{p} - \boldsymbol{p}_r(t)$. Then a possible Proportional/Integral/Derivative (PID) function $\boldsymbol{\xi}$ yielding the exponential stabilization at zero of the extended state error $(\tilde{\boldsymbol{p}}, \tilde{\boldsymbol{v}}, \boldsymbol{I})$ is

$$\boldsymbol{\xi}(\boldsymbol{p}, \boldsymbol{v}, \boldsymbol{I}, t) = \dot{\boldsymbol{v}}_r(t) - k_p (\boldsymbol{p} - \boldsymbol{p}_r(t)) - k_v (\boldsymbol{v} - \boldsymbol{v}_r(t)) - k_I \boldsymbol{I},$$

with k_p, k_v and k_I denoting positive gainss adequately chosen. Of course, the above mentioned functions $\boldsymbol{\xi}$ can be adapted to satisfy complementary constraints (uniform boundedness of the aircraft speed, for instance [8]).

In the case of the *path following* problem, objectives are dual: i) convergence of the aircraft speed $|v|$ (or $|v_a|$, or $|v_{a,1}|$) to a desired speed value v^*, and ii) convergence to zero of the distance between the aircraft position and a pre-defined geometric path. Let ξ_v denote a function such that the equality $|v| = \xi_v(|v|, v^*, I_v, t)$ yields the realization of the first objective. The second objective involves the aircraft heading vector $\boldsymbol{h} = \frac{\boldsymbol{v}}{|v|}$, its angular velocity $\boldsymbol{\omega}_h = \boldsymbol{h} \times \dot{\boldsymbol{h}}$, and the determination of a desired heading vector $\boldsymbol{h}^*$ such that the equality $\boldsymbol{h} = \boldsymbol{h}^*(\boldsymbol{p}, |v|, t)$ yields the exponential stabilization at zero of the distance between the aircraft and the chosen path, provided that the aircraft speed is always larger than some positive value. This latter sub-problem is commonly referred to as the *guidance* problem in the specialized literature. Then, let $\bar{\boldsymbol{\omega}}_h$ denote a function of the orientation error $\boldsymbol{h} \times \boldsymbol{h}^*$ (and possibly other variables) such that the equality $\boldsymbol{\omega}_h = \Pi_h \bar{\boldsymbol{\omega}}_h$ yields the convergence of $\boldsymbol{h}$ to $\boldsymbol{h}^*$ and, subsequently the realization of the second objective. Examples of functions ξ_v and $\bar{\boldsymbol{\omega}}_h$ endowed with the above mentioned properties

are given in [9]. Then a function $\boldsymbol{\xi}$ yielding the achievement of both objectives, when $\dot{\boldsymbol{v}} = \boldsymbol{\xi}$, is

$$\boldsymbol{\xi} = \xi_v \boldsymbol{h} + |v|(\bar{\boldsymbol{\omega}}_h \times \boldsymbol{h}).$$

Indeed, $\boldsymbol{v} = |v|\boldsymbol{h}$ so that $\dot{\boldsymbol{v}} = \dot{|v|}\boldsymbol{h} + |v|(\boldsymbol{\omega}_h \times \boldsymbol{h})$. Using the expression of $\boldsymbol{\xi}$ in the equality $\dot{\boldsymbol{v}} = \boldsymbol{\xi}$ then yields $\dot{|v|} = \xi_v$ and $\boldsymbol{\omega}_h = \Pi_h \bar{\boldsymbol{\omega}}_h$.

2) Second step: This step consists in determining the thrust T, the tilt angle θ, and the aircraft frame $\mathcal{B} = \{G; \boldsymbol{\imath}, \boldsymbol{\jmath}, \boldsymbol{k}\}$, such that

$$m\boldsymbol{\xi} = m\boldsymbol{g} + \boldsymbol{F}_a + T(\sin(\theta)\boldsymbol{\imath} - \cos(\theta)\boldsymbol{k}) \tag{9}$$

The reason is that, in view of (4), the realization of this equality yields $\dot{\boldsymbol{v}} = \boldsymbol{\xi}$. Let us define

$$\begin{array}{l} \boldsymbol{a} := m(\boldsymbol{\xi} - \boldsymbol{g}) \\ \boldsymbol{d} := \boldsymbol{a} + c_0|v_a|\boldsymbol{v}_a \\ \boldsymbol{e} := \boldsymbol{a} + \bar{c}_0|v_a|\boldsymbol{v}_a \end{array} \tag{10}$$

Regrouping (9) and (7) then yields

$$\begin{array}{l} \big(\boldsymbol{d}\cdot\boldsymbol{\imath} - T\sin(\theta)\big)\boldsymbol{\imath} + \big(\boldsymbol{e}\cdot\boldsymbol{k} + T\cos(\theta)\big)\boldsymbol{k} \\ +(\boldsymbol{a}\cdot\boldsymbol{\jmath})\boldsymbol{\jmath} - (\boldsymbol{v}_a\cdot\boldsymbol{\jmath})\boldsymbol{O}(\boldsymbol{v}_a) = \boldsymbol{0} \end{array} \tag{11}$$

To satisfy this equality it is sufficient to define

$$\boldsymbol{\jmath} = \frac{\boldsymbol{v}_a \times \boldsymbol{a}}{|\boldsymbol{v}_a \times \boldsymbol{a}|} \tag{12}$$

and impose

$$\begin{array}{l} \boldsymbol{d}\cdot\boldsymbol{\imath} = T\sin(\theta) \\ \boldsymbol{e}\cdot\boldsymbol{k} = -T\cos(\theta) \end{array} \tag{13}$$

Note that this choice of $\boldsymbol{\jmath}$ corresponds to adopting a so-called "balanced flight" without "sideslip", i.e. for which $\boldsymbol{v}_a \cdot \boldsymbol{\jmath} = 0$. This choice also explains the non-necessity of better modeling in (7) the component of aerodynamic forces acting sideways on the aircraft. Now, the two equalities in (13) are equivalent to

$$T = \sin(\theta)(\boldsymbol{d}\cdot\boldsymbol{\imath}) - \cos(\theta)(\boldsymbol{e}\cdot\boldsymbol{k}) \tag{14}$$

and

$$\tan(\theta) = -\frac{\boldsymbol{d}\cdot\boldsymbol{\imath}}{\boldsymbol{e}\cdot\boldsymbol{k}} \tag{15}$$

Therefore, with $\boldsymbol{\jmath}$ given by (12), the thrust is calculated according to (14), while the tilt angle θ and the vectors $\boldsymbol{\imath}$ and $\boldsymbol{k}$ must satisfy (15). This latter constraint can be exploited in essentially two ways, namely either by imposing the tilt angle value (as a function of time, for instance) and working out unitary vectors $\boldsymbol{\imath}$ and $\boldsymbol{k}$ that satisfy the constraint, or by calculating the tilt angle according to (15) and using a complementary criterion to determine these unitary vectors. The criterion that we propose to consider is the minimization of the thrust $|T|$ which is the main source of energy expenditure. These two possibilities are explored next.

Case 1: imposed tilt angle $\theta(t)$

Conventional fixed-wing aircraft, for which θ is constant and close to $\pi/2$, are covered by this case. This case also covers *ad hoc* tilt-angle monitoring strategies for the transition between hovering and cruising flight, consisting in switching rapidly between zero (hovering) and $\pi/2$ (cruising).

Let us determine $\boldsymbol{\imath}$ and $\boldsymbol{k}$ that satisfy (15). Along a balanced flight the vector $\boldsymbol{\imath}$ is related to the air-velocity via the relation

$$\boldsymbol{\imath} = rot(\alpha\boldsymbol{\jmath})\frac{\boldsymbol{v}_a}{|v_a|} \tag{16}$$

with α denoting the angle of attack, and $rot(\alpha\boldsymbol{\jmath})\boldsymbol{u}$ the rotation of vector $\alpha\boldsymbol{\jmath}$ applied to the unitary vector $\boldsymbol{u}$. From Rodrigues formula and the orthogonality of $\boldsymbol{v}_a$ and $\boldsymbol{\jmath}$

$$\boldsymbol{\imath} = \cos(\alpha)\frac{\boldsymbol{v}_a}{|v_a|} + \sin(\alpha)(\boldsymbol{\jmath} \times \frac{\boldsymbol{v}_a}{|v_a|}) \tag{17}$$

Therefore, using the definition of $\boldsymbol{d}$ (relation (10))

$$\boldsymbol{d}\cdot\boldsymbol{\imath} = (\boldsymbol{a} + c_0|v_a|\boldsymbol{v}_a)\cdot\big(\cos(\alpha)\frac{\boldsymbol{v}_a}{|v_a|} + \sin(\alpha)(\boldsymbol{\jmath}\times\frac{\boldsymbol{v}_a}{|v_a|})\big)$$

This relation may also be written as

$$\begin{array}{l} \boldsymbol{d}\cdot\boldsymbol{\imath} = \cos(\alpha)w_1 + \sin(\alpha)w_2 \\ w_1 := \boldsymbol{a}\cdot\frac{\boldsymbol{v}_a}{|v_a|} + c_0|v_a|^2 \\ w_2 := \boldsymbol{a}\cdot\frac{\boldsymbol{\jmath}\times\boldsymbol{v}_a}{|v_a|} = \frac{|\boldsymbol{v}_a\times\boldsymbol{a}|}{|v_a|} \end{array} \tag{18}$$

The last frame vector $\boldsymbol{k}$ is the the cross product of the other two frame vectors

$$\begin{array}{rcl} \boldsymbol{k} & = & \boldsymbol{\imath}\times\boldsymbol{\jmath} \\ & = & \big(\cos(\alpha)\frac{\boldsymbol{v}_a}{|v_a|} + \sin(\alpha)(\boldsymbol{\jmath}\times\frac{\boldsymbol{v}_a}{|v_a|})\big)\times\boldsymbol{\jmath} \\ & = & \cos(\alpha)\frac{\boldsymbol{v}_a\times\boldsymbol{\jmath}}{|v_a|} + \sin(\alpha)\frac{\boldsymbol{v}_a}{|v_a|} \end{array} \tag{19}$$

Using the definition of $\boldsymbol{e}$ (relation (10))

$$\boldsymbol{e}\cdot\boldsymbol{k} = (\boldsymbol{a} + \bar{c}_0|v_a|\boldsymbol{v}_a)\cdot\boldsymbol{k}$$

and using the expression (19) of $\boldsymbol{k}$

$$\begin{array}{lll} \boldsymbol{e}\cdot\boldsymbol{k} = \cos(\alpha)w_3 + \sin(\alpha)w_4 & & \\ w_3 := \boldsymbol{a}\cdot\frac{\boldsymbol{v}_a\times\boldsymbol{\jmath}}{|v_a|} & = -w_2 & \\ w_4 := \boldsymbol{a}\cdot\frac{\boldsymbol{v}_a}{|v_a|} + \bar{c}_0|v_a|^2 & = w_1 + 2c_1|v_a|^2 & \end{array} \tag{20}$$

Replacing $\boldsymbol{d}\cdot\boldsymbol{\imath}$ and $\boldsymbol{e}\cdot\boldsymbol{k}$ by their expressions (18) and (20) in (15), which may also be written as $\cos(\theta)\boldsymbol{d}\cdot\boldsymbol{\imath} + \sin(\theta)\boldsymbol{e}\cdot\boldsymbol{k} = 0$, yields

$$\begin{array}{l} \cos(\theta)\big(\cos(\alpha)w_1 + \sin(\alpha)w_2\big) \\ +\sin(\theta)\big(\cos(\alpha)w_3 + \sin(\alpha)w_4\big) = 0 \end{array}$$

or, equivalently

$$\begin{array}{rcl} \tan(\alpha) & = & \frac{\sin(\theta)w_2 - \cos(\theta)w_1}{\cos(\theta)w_2 + \sin(\theta)w_4} \\ & = & \frac{\sin(\theta)|\boldsymbol{v}_a\times\boldsymbol{a}| - \cos(\theta)(\boldsymbol{a}\cdot\boldsymbol{v}_a + c_0|v_a|^3)}{\cos(\theta)|\boldsymbol{v}_a\times\boldsymbol{a}| + \sin(\theta)(\boldsymbol{a}\cdot\boldsymbol{v}_a + \bar{c}_0|v_a|^3)} \end{array} \tag{21}$$

The vectors $\boldsymbol{\imath}$ and $\boldsymbol{k}$ are thus given by (17) and (19) with the angle of attack α given by (21). They are uniquely defined provided that i) $|v_a|$ and $|\boldsymbol{v}_a \times \boldsymbol{a}|$ are different from zero, ii) the numerator and denominator in the right member of (21) are not simultaneously equal to zero, i.e. $|\boldsymbol{v}_a \times \boldsymbol{a}|^2 + (\boldsymbol{d}\cdot\boldsymbol{v}_a)(\boldsymbol{e}\cdot\boldsymbol{v}_a) \neq 0$, and iii) neither θ nor $\boldsymbol{\xi}$ depends on the aircraft attitude (to ensure that the previous expressions defining the frame vectors $\boldsymbol{\imath}$, $\boldsymbol{\jmath}$, $\boldsymbol{k}$ are explicit).

In the particular case of a standard fixed-wing aircraft with the thrust direction aligned with $\boldsymbol{\imath}$, i.e. when $\theta = \pi/2$,

one easily verifies that these relations yield $\boldsymbol{\imath} = \frac{\boldsymbol{e}}{|e|}$ when $|e| \neq 0$. If $\theta = 0$, then one also verifies that $\boldsymbol{k} = -\frac{\boldsymbol{d}}{|d|}$ when $|d| \neq 0$.

Case 2: thrust minimization with θ calculated according to (15)
From (14) and (15) one deduces that

$$T^2 = (\boldsymbol{d}\cdot\boldsymbol{\imath})^2 + (\boldsymbol{e}\cdot\boldsymbol{k})^2 \tag{22}$$

Therefore the minimization of $|T|$ is equivalent to the minimization of $(\boldsymbol{d}\cdot\boldsymbol{\imath})^2 + (\boldsymbol{e}\cdot\boldsymbol{k})^2$. In view of (18) and (20)

$$\begin{array}{rcl}(\boldsymbol{d}\cdot\boldsymbol{\imath})^2 + (\boldsymbol{e}\cdot\boldsymbol{k})^2 & = & \big(\cos(\alpha)w_1 + \sin(\alpha)w_2\big)^2 \\ & & +\big(\cos(\alpha)w_3 + \sin(\alpha)w_4\big)^2\end{array}$$

so that

$$\begin{array}{rcl}\frac{\partial}{\partial\alpha}\left((\boldsymbol{d}\cdot\boldsymbol{\imath})^2 + (\boldsymbol{e}\cdot\boldsymbol{k})^2\right) & = & \sin(2\alpha)(w_2^2 + w_4^2 - w_1^2 - w_3^2) \\ & & +2\cos(2\alpha)(w_1w_2 + w_3w_4) \\ & = & -\sin(2\alpha)(4w_1c_1|v_a|^2 + 4c_1^2|v_a|^4) \\ & & +2\cos(2\alpha)(2c_1w_2|v_a|^2)\end{array}$$

The minimizing angle of attack is obtained by zeroing the right-hand side of this equality, i.e. when either $\boldsymbol{v}_a = 0$, in which case the angle of attack is undetermined and T is necessarily equal to the aircraft weight mg_0, or $\boldsymbol{v}_a \neq 0$ and

$$\begin{array}{rcl}\tan(2\alpha) & = & \frac{w_2}{w_1 + c_1|v_a|^2} \\ & = & \frac{|\boldsymbol{v}_a\times\boldsymbol{a}|}{\boldsymbol{a}\cdot\boldsymbol{v}_a + (c_0+c_1)|v_a|^3}\end{array} \tag{23}$$

The optimal angle of attack is then given by

$$\alpha = 0.5\ \text{atan2}(|\boldsymbol{v}_a\times\boldsymbol{a}|, \boldsymbol{a}\cdot\boldsymbol{v}_a + (c_0+c_1)|v_a|^3) \tag{24}$$

with α smaller than $\pi/4$ when $(\boldsymbol{g}-\boldsymbol{\xi})\cdot\boldsymbol{v}_a < 0$, even at low airspeeds. This latter value is noticeable because it does not depend on the aircraft aerodynamic characteristics. It is thus, in particular, independent of the loss of lift associated with stall at low airspeeds in (quasi) horizontal flight. The vectors $\boldsymbol{\imath}$ and $\boldsymbol{k}$ are still given by (17) and (19) with the angle of attack α now given by (24), and the tilt angle calculated according to (15).

3) Third step: The aircraft orientation specified by the unitary vectors $\boldsymbol{\imath}$, $\boldsymbol{\jmath}$, $\boldsymbol{k}$ determined at the previous step should be regarded as a desired orientation that the aircraft orientation control system has to asymptotically stabilize. To distinguish these vectors from the actual aircraft body-frame vectors, we now denote them as $\bar{\boldsymbol{\imath}}$, $\bar{\boldsymbol{\jmath}}$, $\bar{\boldsymbol{k}}$. Therefore,

$$\begin{array}{l}\bar{\boldsymbol{\jmath}} = \frac{\boldsymbol{v}_a\times\boldsymbol{a}}{|\boldsymbol{v}_a\times\boldsymbol{a}|} \\ \bar{\boldsymbol{\imath}} = \cos(\alpha)\frac{\boldsymbol{v}_a}{|v_a|} + \sin(\alpha)(\bar{\boldsymbol{\jmath}}\times\frac{\boldsymbol{v}_a}{|v_a|}) \\ \bar{\boldsymbol{k}} = \bar{\boldsymbol{\imath}}\times\bar{\boldsymbol{\jmath}}\end{array} \tag{25}$$

with the angle of attack α given either by (21), if the tilt angle $\theta(t)$ is imposed, or by (24), when a complementary objective is the minimization of the thrust. In this latter case the tilt angle is calculated according to (15).
The last control design step then consists in determining $\boldsymbol{\omega}$ that makes the actual aircraft frame $\mathcal{B} = \{G; \boldsymbol{\imath}, \boldsymbol{\jmath}, \boldsymbol{k}\}$ converge to the desired frame $\bar{\mathcal{B}} = \{G; \bar{\boldsymbol{\imath}}, \bar{\boldsymbol{\jmath}}, \bar{\boldsymbol{k}}\}$. To this aim, and for this latter problem to be well conditioned, it matters to verify that the orientation of $\bar{\mathcal{B}}$ does not depend on the aircraft attitude. In particular, and as already mentioned, the feedback vector $\boldsymbol{\xi}$ associated with the main control objectives should not depend on the aircraft attitude. Let us then denote the angular velocities of $\bar{\boldsymbol{\imath}}$ and $\bar{\boldsymbol{\jmath}}$ w.r.t. the inertial frame as $\boldsymbol{\omega}_{\bar{\boldsymbol{\imath}}} := \bar{\boldsymbol{\imath}}\times\dot{\bar{\boldsymbol{\imath}}}$ and $\boldsymbol{\omega}_{\bar{\boldsymbol{\jmath}}} := \bar{\boldsymbol{\jmath}}\times\dot{\bar{\boldsymbol{\jmath}}}$ respectively. Since $\bar{\boldsymbol{\imath}}$ and $\bar{\boldsymbol{\jmath}}$ do not depend on the aircraft orientation, their time-derivatives do not depend on the aircraft angular velocity $\boldsymbol{\omega}$. The angular velocity of the frame $\bar{\mathcal{B}}$ is then given by $\bar{\boldsymbol{\omega}} = \boldsymbol{\omega}_{\bar{\boldsymbol{\imath}}} + (\bar{\boldsymbol{\imath}}.\boldsymbol{\omega}_{\bar{\boldsymbol{\jmath}}})\bar{\boldsymbol{\imath}} = \boldsymbol{\omega}_{\bar{\boldsymbol{\jmath}}} + (\bar{\boldsymbol{\jmath}}.\boldsymbol{\omega}_{\bar{\boldsymbol{\imath}}})\bar{\boldsymbol{\jmath}}$, and this velocity does not depend on $\boldsymbol{\omega}$ either. An angular velocity $\boldsymbol{\omega}$ that almost globally asymptotically (locally exponentially) stabilizes $\mathcal{B} = \bar{\mathcal{B}}$ is, for instance (see [10])

$$\boldsymbol{\omega} = \bar{\boldsymbol{\omega}} + k_\omega(t)\big((\boldsymbol{\imath}\times\bar{\boldsymbol{\imath}}) + (\boldsymbol{\jmath}\times\bar{\boldsymbol{\jmath}}) + (\boldsymbol{k}\times\bar{\boldsymbol{k}})\big) \tag{26}$$

with $k_\omega(t) > \epsilon > 0$.

B. Control at low airspeeds

When $|v_a| = 0$ the aircraft wings do not produce lift (nor drag) and the control design reported in the previous section does not apply due to the singularity arising for the definition of the desired aircraft-fixed frame. This frame thus has to be defined in a different way when $|v_a|$ tends to become small, i.e. when the aerodynamic forces acting on the aircraft tend to vanish. Then $\boldsymbol{a} \approx \boldsymbol{d} \approx \boldsymbol{e}$. When $\boldsymbol{F}_a = \boldsymbol{0}$, relation (9) simplifies to

$$\boldsymbol{a} = T(\sin(\theta)\boldsymbol{\imath} - \cos(\theta)\boldsymbol{k}) \tag{27}$$

which in turn implies $\boldsymbol{a}\cdot\boldsymbol{\jmath} = 0$,

$$T = \sin(\theta)(\boldsymbol{a}\cdot\boldsymbol{\imath}) - \cos(\theta)(\boldsymbol{a}\cdot\boldsymbol{k}) \tag{28}$$

and

$$\tan(\theta) = -\frac{\boldsymbol{a}\cdot\boldsymbol{\imath}}{\boldsymbol{a}\cdot\boldsymbol{k}} \tag{29}$$

These relations also imply $T = \pm|a|$. They can be satisfied in many ways. Let us just mention two simple options for the choice of the desired aircraft-fixed frame vectors.
Option 1: vertical aircraft body

$$\bar{\boldsymbol{\imath}} = \frac{\boldsymbol{a}}{|a|},\ \theta = \pi/2,\ T = |a|.$$

Option 2: horizontal aircraft body

$$\bar{\boldsymbol{k}} = -\frac{\boldsymbol{a}}{|a|},\ \theta = 0,\ T = |a|.$$

Both options implicitly yield $\boldsymbol{a}\cdot\bar{\boldsymbol{\jmath}} = 0$ so that it is not "strictly necessary" to further specify the vector $\bar{\boldsymbol{\jmath}}$, nor the third frame vector. Possible angular velocity control laws associated with these options are

$$\boldsymbol{\omega} = \boldsymbol{\omega}_{\bar{\boldsymbol{k}}} + k_\omega(t)(\boldsymbol{k}\times\bar{\boldsymbol{k}}) \tag{30}$$

and

$$\boldsymbol{\omega} = \boldsymbol{\omega}_{\bar{\boldsymbol{\imath}}} + k_\omega(t)(\boldsymbol{\imath}\times\bar{\boldsymbol{\imath}}) \tag{31}$$

respectively. Since $\boldsymbol{a} = -m\boldsymbol{g}$ when $\boldsymbol{v}_a = \boldsymbol{0}$ and $\boldsymbol{\xi} = 0$, the first option corresponds to having the aircraft nose up at low airspeeds, alike a tail-sitter, whereas the second one

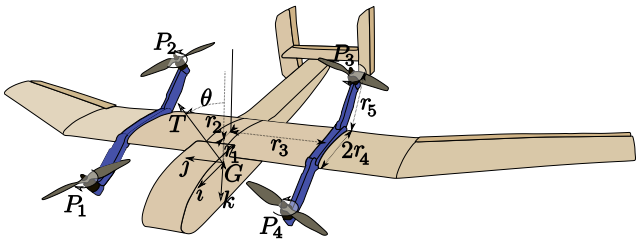

Fig. 2. Example of a quad tilt rotor configuration

corresponds to maintaining the aircraft body approximately horizontal.

To further enforce a small sideslip angle as soon as the airspeed is different from zero, one may complement both options with a "pseudo" frame vector $\bar{\bar{\boldsymbol{j}}} = \frac{\boldsymbol{v}_a \times \boldsymbol{a}}{|\boldsymbol{v}_a \times \boldsymbol{a}| + \epsilon}$, with ϵ denoting a small positive number added to the denominator to avoid indetermination when $|\boldsymbol{v}_a \times \boldsymbol{a}| = 0$. Note that using this vector in (26) is equivalent to using the unitary vector $\bar{\boldsymbol{j}} = \frac{\boldsymbol{v}_a \times \boldsymbol{a}}{|\boldsymbol{v}_a \times \boldsymbol{a}|}$ multiplied by the varying gain $\frac{|\boldsymbol{v}_a \times \boldsymbol{a}|}{|\boldsymbol{v}_a \times \boldsymbol{a}| + \epsilon}$. The "pseudo" desired frame is then complemented with the vector $\bar{\bar{\boldsymbol{k}}} = \bar{\boldsymbol{i}} \times \bar{\bar{\boldsymbol{j}}}$ (resp. $\bar{\bar{\boldsymbol{i}}} = \bar{\bar{\boldsymbol{j}}} \times \bar{\boldsymbol{k}}$) in the case of the first (resp. second) option. A possible angular velocity control law is then given by (26). As for the thrust T and the tilt angle θ, they continue to be calculated by using the relations (14) and (15).

It then remains to work out a transition law, based on the measured airspeed intensity, that smoothly mixes the attitude control laws proposed in this section with those proposed in Section III-A, when airspeed and aerodynamic forces are not small. For instance, let $\boldsymbol{\omega}_1$ (resp. $\boldsymbol{\omega}_2$) denote the chosen angular velocity control law when the airspeed is not (resp. is) small, and v^* the chosen airspeed transition value. Then a possible angular velocity control law is

$$\boldsymbol{\omega} = \lambda(|v_a|)\boldsymbol{\omega}_1 + (1 - \lambda(|v_a|)\boldsymbol{\omega}_2$$

with λ a non-decreasing smooth function on $\mathbb{R}^+$ such that $\lambda(x) = 0$ when $0 \leq x < v^* - \epsilon$, and $\lambda(x) = 1$ when $x > v^* + \epsilon$, with ϵ denoting a small positive number. The size of v^* can vary in large proportions, depending typically on the aircraft aerodynamic properties and the criterion for the occurrence of the transition between hovering and cruising flight.

IV. Actuation of a quad tilt rotor aircraft

Let $\boldsymbol{\omega}^*$ denote the desired aircraft angular velocity (derived according the methodology proposed in the preceding section, for instance), and let $\boldsymbol{\Gamma}$ denote a control torque vector in charge of ensuring the (near) asymptotic stabilization at zero of the angular velocity error $\omega - \omega^*$. In view of the classical Newton-Euler equation

$$J\dot{\omega} = J\omega \times \omega + \Gamma \ (+\text{parasitic terms}) \tag{32}$$

with J denoting the aircraft inertia matrix, a simple possibility consists in setting

$$\Gamma = -k_\gamma J(\omega - \omega^*) + \omega \times J\omega^* \tag{33}$$

with $k_\gamma > 0$ denoting a large control gain. In the case of a quad tilt rotor aircraft, like the one represented in Fig. 1, this control torque can be produced either by the four propellers (using differential multi-rotors speeds), or by the moving (ailerons/rudder/elevator) control surfaces of the aircraft, or by a combination of the two systems, i.e.

$$\Gamma = \Gamma_m + \Gamma_a \tag{34}$$

with Γ_m the torque vector produced by the set of propellers, and Γ_a the torque vector produced by the aircraft moving surfaces.

Now, given a desired control torque vector Γ, an issue is to distribute the torque production between the two systems knowing that at low airspeeds moving control surfaces are inefficient, and that at high airspeeds they typically produce torques more effectively than the propellers. A possibility is to set

$$\Gamma_a = \bar{\lambda}(|v_a|)\Gamma \ , \ \Gamma_m = \big(1 - \bar{\lambda}(|v_a|)\big)\Gamma \tag{35}$$

with $\bar{\lambda}$ a non-decreasing smooth function on $\mathbb{R}^+$ such that $\bar{\lambda}(x) = 0$ when $0 \leq x < \bar{v}^* - \bar{\epsilon}$, and $\bar{\lambda}(x) = 1$ when $x > \bar{v}^* + \bar{\epsilon}$, with ϵ denoting a small positive number. Note that an interest of such a distribution is to use the propellers essentially for the sole production of thrust at high airspeeds, thus limiting the differences and variations of the multi-rotors speeds. This goes with less wear of the motors, and better energy efficiency.

It remains to determine the tilting angles δ_j $(j = 1, 2, 3)$ of the moving control surfaces in charge of producing Γ_a, and the propeller's angular velocities w_i $(i = 1, 2, 3, 4)$ in charge of producing (T, Γ_m).

The first of these issues is classically solved by calculating the angle vector $\delta = [\delta_1, \delta_2, \delta_3]^\top$ via a relation of the form

$$\delta = \frac{1}{|v_a|^2} A\Gamma_a \tag{36}$$

with the components of the matrix A depending primarily on the size of the control surfaces, and on their placement w.r.t. the aircraft CoM.

Concerning the second issue, for articulated quad tilt rotor systems, like the one represented in Fig. 2, the thrust intensity T and torque Γ_m are related to the propellers rotor speeds w_i $(i = 1, 2, 3, 4)$ via a relation of the form

$$\begin{bmatrix} T \\ \Gamma_m \end{bmatrix} = D(\theta) \begin{bmatrix} \mu w_1^2 \\ \mu w_2^2 \\ \mu w_3^2 \\ \mu w_4^2 \end{bmatrix} \tag{37}$$

with μ denoting the positive ratio (thrust intensity over squared rotor speed) of each propeller,

$$D(\theta) = D_1(\theta) D_2 \ , \ D_2 = \begin{bmatrix} 1 & 1 & 1 & 1 \\ 1 & -1 & -1 & 1 \\ 1 & 1 & -1 & -1 \\ 1 & -1 & 1 & -1 \end{bmatrix} \tag{38}$$

and $D_1(\theta)$ depending on the tilt angle and the position of the propellers w.r.t. the aircraft CoM. For instance, in the particular case of the quad tilt rotor aircraft represented in Fig. 2,

$$D_1(\theta) = \begin{bmatrix} 1 & 0 & 0 & 0 \\ 0 & 0 & -r_3 c_\theta & -\frac{\nu}{\mu} s_\theta \\ r_1 c_\theta + r_2 s_\theta & r_4 c_\theta + r_5 & 0 & 0 \\ 0 & 0 & -r_3 s_\theta & \frac{\nu}{\mu} c_\theta \end{bmatrix} \quad (39)$$

with ν denoting the positive ratio (anti-torque intensity over squared rotor speed) of each propeller. In the preceding relation we have used the notation c_θ and s_θ for $\cos(\theta)$ and $\sin(\theta)$ respectively. Because the matrix D_2 is invertible, and the matrix $D_1(\theta)$ is invertible in a large range of tilting angles (comprising the interval $[0, \pi/2]$), the product matrix $D(\theta)$ is also invertible in this range of angles. $D_1(\theta)$ is in fact invertible for all tilting angles if $r_5 > r_4$, but this is of little practical relevance because of the physical limitations of the tilting mechanism. Define $X := [\mu w_1^2, \mu w_2^2, \mu w_3^2, \mu w_4^2]^\top$. Relation (37) suggests to calculate the rotor speeds via the inversion of the matrix $D(\theta)$, i.e.

$$X = D^{-1}(\theta) \begin{bmatrix} T \\ \Gamma_m \end{bmatrix}$$

A known difficulty is that it is not certain that the components of the vector X so obtained are all positive, nor that they are smaller than the maximal force μw_{max}^2 that a rotor can produce.

V. Hardware-in-the-loop simulation

The object of this section is to test the control approach reported in the previous sections in the case of a trajectory tracking problem. The proposed control laws are implemented on a commercially available "Pixhawk 3 Pro" autopilot flight controller. The code implementation is based on the open-source PX4 flight stack [12]. To perform hardware-in-the-loop simulations, this hardware is connected to a flight simulator. We use the Gazebo robot simulator, along with open source plugins (based on the RotorS Project) whose purpose is to simulate UAV models and interface them with the controller hardware (https://github.com/PX4/sitl_gazebo). The aircraft model used for this simulation mimics a 2.5 kg tilt-rotor fixed-wing drone, alike the one shown in Fig 1.

The flight mode transition airspeed v^* is set equal to 4 m/s, and the airspeed $\bar{v}^*$ for the torque production transition (between the rotors and the control surfaces) is set equal to 7 m/s. The tilt angle θ is bound to remain in the interval $[0, \pi/2]$ and is calculated to minimize the thrust intensity, as explained in Section III-A.2. At low airspeeds the objective is to keep the aircraft fuselage horizontal (see Section III-B). For this simulation there is no wind so that $\boldsymbol{v}_a = \boldsymbol{v}$.

The chosen reference trajectory (see Figures 3 and 4) consists of an ascending phase, at an airspeed of 2 m/s, followed by a horizontal flight along a straight line during which the reference speed increases from 0 m/s to 10 m/s.

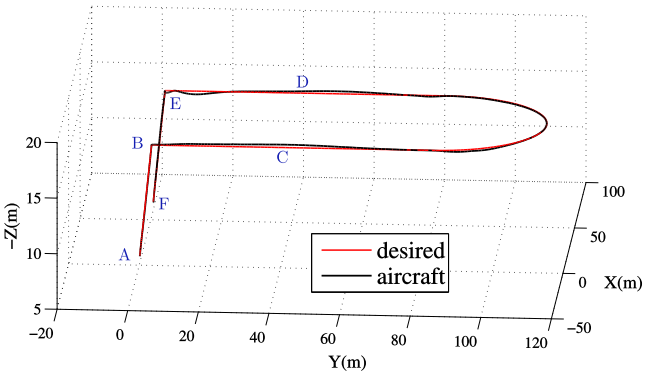

Fig. 3. Trajectories

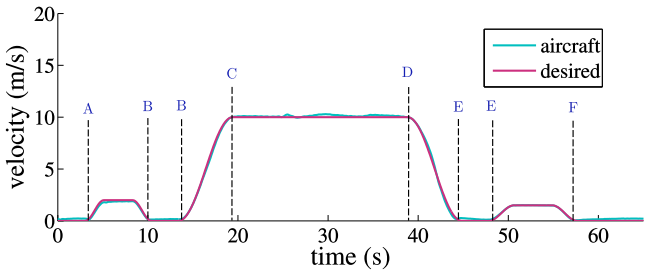

Fig. 4. Velocities

This latter phase highlights a transition between hovering and cruising flight. The trajectory subsequently involves a circular turn with a 30 m radius, followed by a decelerating horizontal flight along a straight line that illustrates a transition from cruising flight to motionless hovering. The trajectory then involves a descent phase at an airspeed of 1.5 m/s, before a final stop.

Figures 3 shows that the vehicle closely follows the reference trajectory. Fig 5 shows the variation of the tilting angle which, as expected, increases from 0 deg, when the aircraft hovers, to 90 deg at high airspeeds. Figures 6 and 7 show the actuators command signals. Control surfaces become active when the longitudinal airspeed exceeds $\bar{v}^*$. The rotors then produce the needed thrust and zero torque.

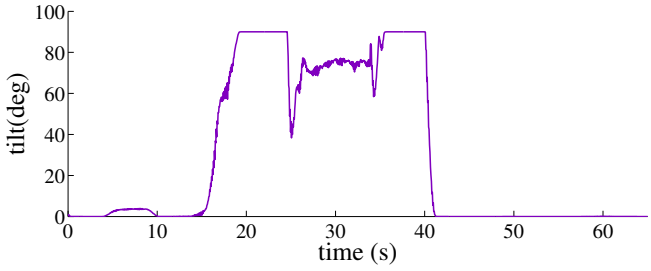

Fig. 5. Rotors tilt angle

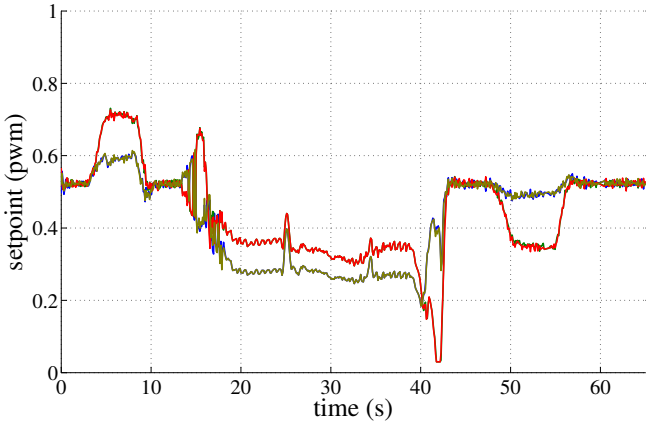

Fig. 6. Rotors thrust command signals

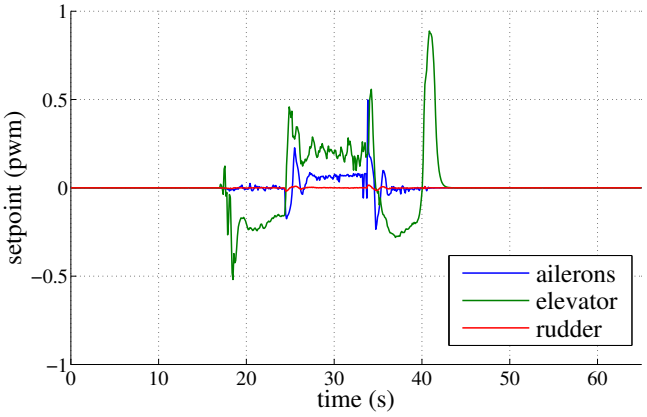

Fig. 7. Control surfaces command signals

VI. Concluding remarks

The proposed control design, and the hardware-in-the-loop simulation reported here, rely on models of aerodynamic forces acting on the aircraft that neglect a certain number of parasitic aerodynamic terms associated with a vectorized thrust mechanism: drag forces on tilted rotors and propellers, interferences between rotors and wings, etc. Even though the aircraft model used for simulation is more elaborate than the one used for control design, which is already useful to credit the control design with some robustness, it does not account for all the phenomena involved in the flight of such a vehicle. Future work should thus focus on the performance impact of non-modeled terms –including actuation limitations–, on improving the control design and robustness with respect to these terms, and on the creation of more advanced models of convertible aircraft for simulation. The allocation of control forces and torques on the different actuation systems also deserves to be more thoroughly studied. And, of course, the proposed control methodology needs to be tested and validated via extensive experimentation on physical convertible aircraft.

References

[1] Z. Liu, Y. He, L. Yang, and J. Han, "Control techniques of tilt rotor unmanned aerial vehicle systems: a review," *Chinese Journal of Aeronautics*, vol. 30, no. 1, pp. 135–148, 2017.

[2] P. Morin, "Modeling and control of convertible micro air vehicles," in *2015 10th International Workshop on Robot Motion and Control (RoMoCo)*, July 2015, pp. 188–198.

[3] A. Ramirez Serrano, "Design methodology for hybrid (vtol + fixed wing) unmanned aerial vehicles," *Aeronautics and Aerospace Open Access Journal*, vol. 2, 06 2018.

[4] S. Yanguo and W. Huanjin, "Design of flight control system for a small unmanned tilt rotor aircraft," *Chinese Journal of Aeronautics*, vol. 22, pp. 250–256, 06 2009.

[5] G. R. Flores-Colunga and R. Lozano-Leal, "A nonlinear control law for hover to level flight for the quad tilt-rotor uav," in *19th IFAC World Congress*, vol. 47, no. 3, August 2014, pp. 11 055–11 059.

[6] G. D. Francesco and M. Mattei, "Modeling and incremental nonlinear dynamic inversion control of a novel unmanned tiltrotor," *Journal of Aircraft*, vol. 53, no. 1, pp. 250–256, 2016.

[7] M. Ciopcia and C. Szczepaski, "Quad-tiltrotor modelling and control," *Journal of Marine Engineering & Technology*, vol. 16, no. 4, pp. 331–336, 2017.

[8] J.-M. Kai, T. Hamel, and C. Samson, "A nonlinear approach to the control of a disc-shaped aircraft," in *IEEE CDC 2017 56th IEEE Conference on Decision and Control*, 2017, pp. 2750–2755.

[9] J. Kai, A. Anglade, T. Hamel, and C. Samson, "Design and experimental validation of a new guidance and flight control system for scale-model airplanes," in *proceedings of 57th IEEE Conference on Decision and Control (CDC)*, Miami, Florida, December 2018, pp. 4270–4276.

[10] J. Kai, T. Hamel, and C. Samson, "A nonlinear global approach to scale-model aircraft path following control," *CoRR*, vol. abs/1803.05184, 2018. [Online]. Available: http://arxiv.org/abs/1803.05184

[11] D. Pucci, T. Hamel, P. Morin, and C. Samson, "Nonlinear feedback control of axisymmetric aerial vehicles," *Automatica*, vol. 53, pp. 72–78, 2015.

[12] L. Meier, D. Honegger, and M. Pollefeys, "Px4: A node-based multithreaded open source robotics framework for deeply embedded platforms," in *2015 IEEE International Conference on Robotics and Automation (ICRA)*, vol. 2015, 2015, pp. 6235–6240.